

A scanning tunneling microscopy study of clean and Cs-covered InSb(110)

L. J. Whitman, Joseph A. Stroscio, R. A. Dragoset, and R. J. Celotta

Electron and Optical Physics Division, National Institute of Standards and Technology, Gaithersburg, Maryland 20899

(Received 24 July 1990; accepted 29 September 1990)

Scanning tunneling microscopy has been employed to study clean and Cs-covered InSb(110) surfaces. Atomic-resolution images of both the filled and empty electronic state densities have been obtained. The surface relaxation determined from these images is in good agreement with that predicted by structure calculations. A variety of surface defects have been observed, with the most common appearing to be simple Sb vacancies. Adjacent In and Sb vacancies (Schottky defects) have also been observed. The perturbation of the surface surrounding these defects is asymmetrical along [001], as might be expected due to the asymmetry in the surface. Surprisingly, the perturbation is also asymmetrical along $[1\bar{1}0]$, where symmetry is expected. Cs adsorbed on room-temperature InSb(110) forms one-dimensional zig-zag chains along $[1\bar{1}0]$, similar to those previously observed on GaAs(110).

I. INTRODUCTION

Indium antimonide (InSb) is an important narrow band-gap semiconductor with applications in near infrared detection¹ and high-speed optoelectronics.² However, relatively few studies of its surfaces have been reported.³⁻¹⁰ The structure of the (110) surface has been investigated with low-energy electron diffraction,^{3,8} and the plasmons and phonons associated with this surface have been studied with electron energy loss spectroscopy.^{6,7} In addition, interface formation between InSb(110) and Ge (Ref. 9) and Se (Ref. 10) has been monitored with synchrotron-radiation photoemission spectroscopy. To our knowledge, the only other InSb surface examined to date is the reconstructed (111)2×2 surface, which has been probed with x-ray diffraction.⁴

In this paper we report a scanning tunneling microscopy (STM) study of clean and Cs-covered InSb(110).¹¹ The InSb(110) surface is interesting to study with STM for a number of reasons. As a polar III-V semiconductor compound, the two dangling bonds broken at the surface are rehybridized into a single lone pair localized on the group-V element, leaving an empty valence orbital on the group-III element.¹² Hence, the occupied surface state density, observed when tunneling from the sample to the STM tip, is concentrated on the group-V anion, and the unoccupied state density, observed when tunneling from tip to sample, is on the group-III cation.¹³⁻¹⁵ This enables atom-selective imaging of the different chemical elements on the surface, as previously reported only on GaAs(110),¹⁶ and facilitates identification of surface defects. Furthermore, atom-selective imaging can be employed to determine the relative positions of the filled and empty dangling bonds within the unit cell, indicative of the degree of surface relaxation at the (110) zinc-blende III-V surface.¹⁶ The relaxation may then be compared with the calculated structure. InSb(110) also offers an interesting template for the adsorption of Cs, which has previously been observed to form long zig-zag chains along the $[1\bar{1}0]$ direction on GaAs(110).^{17,18} With the largest lattice constant of all the zinc-blende III-V semiconduc-

tors (15% larger than GaAs), the effects of lattice constant on Cs chain formation can be most effectively studied with InSb(110).

II. EXPERIMENT

InSb (110)-oriented samples (*n* type, Te doped $1.6\text{--}3.0 \times 10^{15} \text{ cm}^{-3}$) were cleaved *in situ* under ultrahigh vacuum ($< 1 \times 10^{-10}$ Torr) to expose a clean (110) crystal face. Cs was deposited from a getter-type source, and the samples were then mounted on the STM. The STM is an IBM Zurich-type microscope^{19,20}; the sample is mounted on a "louse" for coarse positioning, the tip is mounted on a piezo tripod, and the whole microscope stage is mounted on a glass frame with a double-spring suspension system for vibration isolation. The probe tips were prepared by electrochemically etching (111)-oriented 0.005-in.-diam tungsten wire, and cleaned *in situ* by electron-bombardment heating.

Topographic images were obtained with a constant tunnel current of 0.1 nA, with a typical height resolution of 0.02 Å and lateral resolution < 4 Å. The scan rate was typically 100 Å s⁻¹. Images recorded simultaneously at different bias voltages were obtained by completing one scan line at the first bias, returning the probe tip to the origin, and then switching the bias and recording another scan line at the second bias voltage. In this way the two images will be offset by at most the thermal drift that occurs during the scan of a single line. The images were recorded with the $[1\bar{1}0]$ direction at approximately 45° with respect to the $+x$ scan direction. Those displayed here have not been corrected for the effects of thermal drift (typically 1–2 Å min⁻¹).

III. RESULTS AND DISCUSSION

Prior to describing the STM results it is useful to briefly review the structure of the zinc-blende (110) surface. As illustrated in Fig. 1(a), when viewed from above, the ideal bulk-terminated InSb(110) surface consists of alternating rows of In and Sb atoms. Within the outermost layer the In (or Sb) rows are 6.5 Å apart, with adjacent atoms within

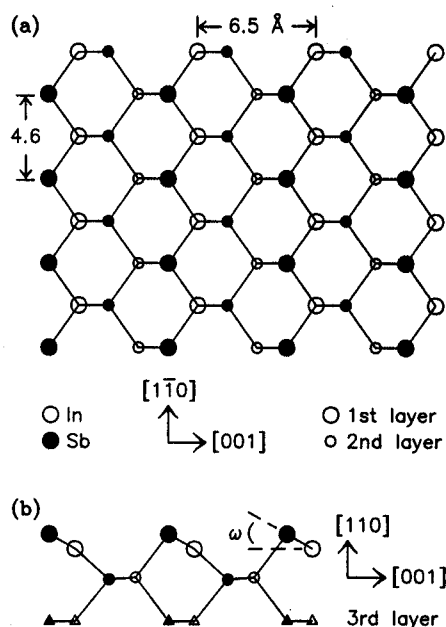
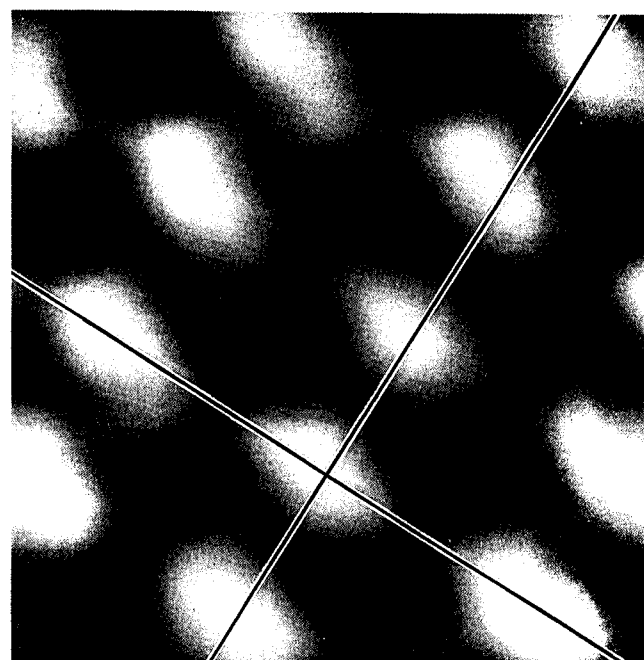


FIG. 1. (a) A top view model of the ideally terminated zinc-blende (110) surface. The symbols represent atom core positions and the lines interatomic bonds. Note that for a given atom the adjacent atoms in either direction along the row are equivalent. In contrast, bonding to the neighboring rows in the $[001]$ direction differs from that along $[00\bar{1}]$. (b) A side view of the first three atomic layers of the (110) surface. The calculated surface relaxation has been included (see Ref. 21), defined by the first layer buckling angle ω .

each row separated by 4.6 \AA . Note that $(1\bar{1}0)$ forms a mirror plane, so that for a given surface atom the neighbors in the $[1\bar{1}0]$ direction are symmetrical with those opposite along $[\bar{1}10]$. In contrast, (001) is *not* a mirror plane; each row of surface atoms is bonded differently to the neighboring rows in the $[001]$ -versus- $[00\bar{1}]$ directions. A side view of the top three layers at the surface is shown in Fig. 1(b), where we have included the calculated surface relaxation. As calculated by Mailhot, Duke, and Chadi,²¹ the Sb buckles outward slightly, resulting in a buckling angle ω of 30° .

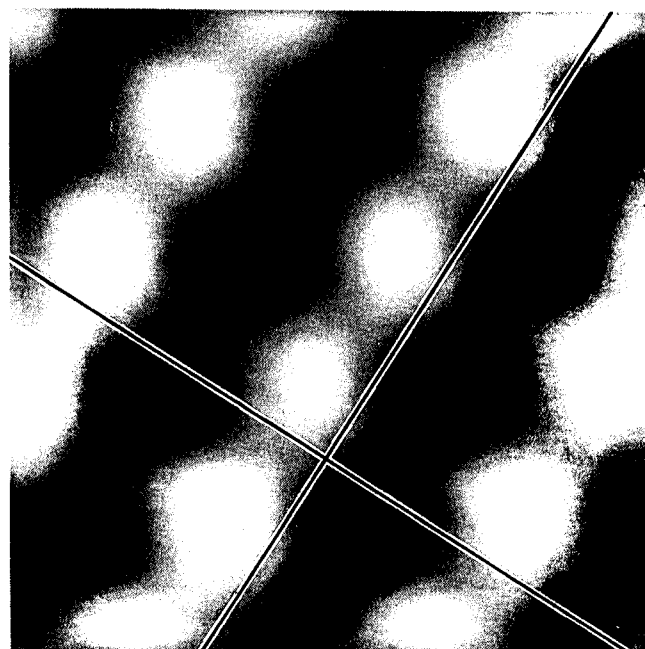
Simultaneously recorded images of the empty and filled state densities on a freshly cleaved surface are displayed in Figs. 2(a) and 2(b), respectively. As made clear by the cross hairs placed in the same location in both images, the empty In state density is shifted with respect to the filled Sb state density. Although there is some variation from image pair to image pair due to tip effects and thermal drift, on average the In and Sb are displaced by half a unit cell along $[1\bar{1}0]$ as expected. Along the $[001]$ direction we find the rows to be separated by $2.4 \pm 0.4 \text{ \AA}$.²² The dependence of the measured filled-versus-empty state density shift on surface buckling angle has been calculated for GaAs(110).¹⁵ Rather than repeat the calculation for InSb, since the structures of InSb and GaAs are so similar we assume that the relative lateral positions of the filled and empty dangling bonds scale with the lattice constant.²³ With this assumption, the shift of 2.4 \AA on InSb(110) occurs for a surface buckling angle of 29° ,²² in good agreement with the calculated buckling.²¹

While scanning the surface with STM, various defects are



(a)

$[1\bar{1}0]$
 $[001]$



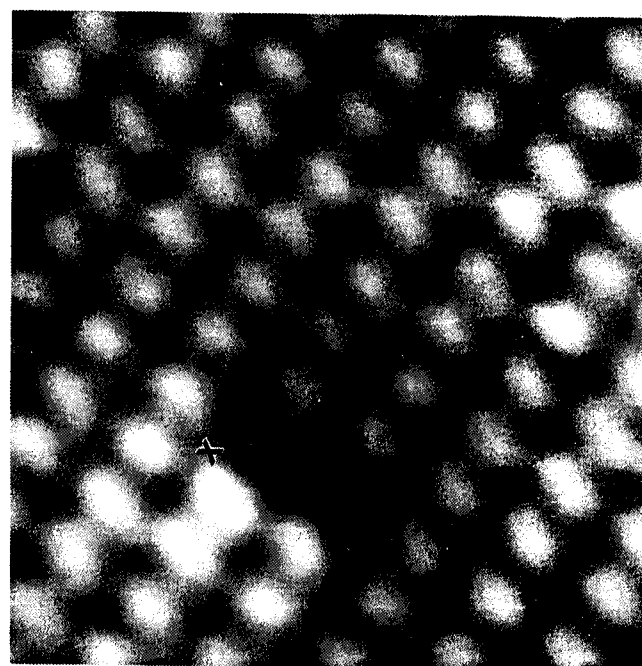
(b)

FIG. 2. A pair of gray-scale topographic images, $17 \times 17 \text{ \AA}$, of a cleaved InSb(110) surface. The images were acquired simultaneously with sample bias voltages of (a) $+1.2$ and (b) -1.0 V. The unoccupied state density concentrated on the In atoms is observed in (a), and the occupied state density concentrated on the Sb atoms is observed in (b). The surface corrugation is $\approx 0.2 \text{ \AA}$ in the $[1\bar{1}0]$ direction (along the rows) and 0.5 \AA along $[001]$ (across the rows) at both biases. The cross marks, displayed in the same location in both images, reveal the relative positions of the In and Sb dangling bonds; on average the Sb is shifted with respect to the In half a unit cell in the $[1\bar{1}0]$ direction and $2.4 \pm 0.4 \text{ \AA}$ along $[001]$. Note that the shift is somewhat smaller than average in this image due to thermal drift and tip effects.

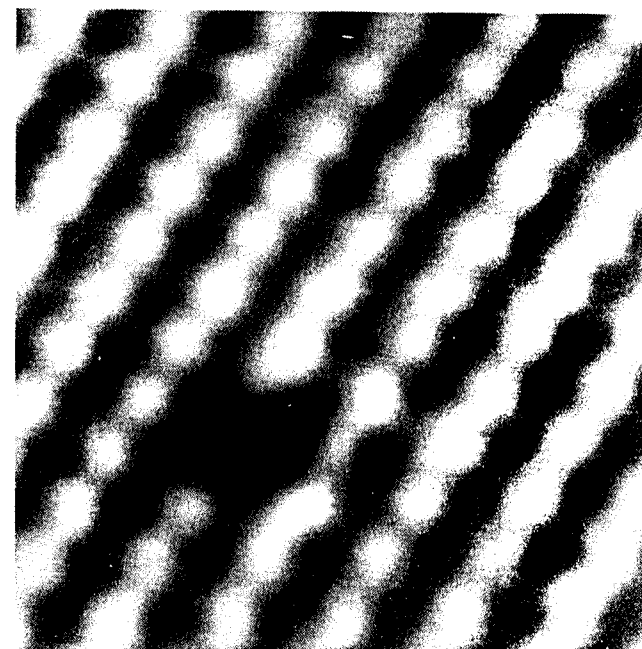
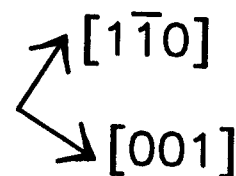
occasionally observed. We estimate their concentration to be between 10^{11} and 10^{13} cm^{-2} , varying from sample to sample and even from region to region on any given sample. The most common type of defect observed appears to be a simple anion (Sb) vacancy, as shown in Fig. 3. Again images of the In and Sb state densities recorded simultaneously are displayed. As seen in the image of the Sb state density [Fig. 3(b)], there appears to be a single missing Sb. The location of this vacancy in the corresponding empty state (In) image [Fig. 3(a)] is indicated by the "×." Substantial vertical and lateral perturbations are observed in the positions of both the empty (In) and filled (Sb) dangling bonds that are within approximately two lattice constants of the defect. If this is truly an anion vacancy the defect should have a local positive charge, and therefore the changes in the apparent "height" of some of the dangling bonds may be due in part to associated charge redistribution (as opposed to outward relaxation of the surface atoms). The lateral displacements, however, should correlate more closely with shifts in the atomic positions at the surface. Note that the neighboring surface atoms on the [001] (right) side of the vacancy [Fig. 3(a)] are more strongly perturbed than those on the $[00\bar{1}]$ side. This is always observed to be the case, and must be related to the underlying asymmetry in the surface; in the [001] direction the first In row has broken bonds, whereas in $[00\bar{1}]$ the In row may only be affected through the back bonds (see Fig. 1). What is peculiar is that the second In row in the [001] direction is also perturbed, though it is also connected to the defect only via back bonds.

Surprisingly, along the rows, where symmetry is expected, surface atoms adjacent to the vacancy are buckled asymmetrically. The relaxation and/or charge redistribution induced in the In atoms adjacent to the missing Sb appears to be polarized across the defect, with the In atom to the upper right of the vacancy ($[1\bar{1}0]$ direction) "lower" and the opposing In "raised." The opposite vertical polarization is observed in the Sb atoms adjacent to the vacancy in the row, though it is difficult to see in the gray-scale image. Since there is nothing to define the direction of this asymmetrical buckling along the row, one might expect its occurrence in either direction with respect to a vacancy. This is indeed the case; some anion vacancies are observed with the opposite polarization, i.e., with the In adjacent in the $[1\bar{1}0]$ direction raised and the opposing In lower.

Dual vacancies, where adjacent In and Sb surface atoms appear to be missing, are also observed, though with less frequency than single Sb vacancies. Images of one such Schottky defect²⁴ are displayed in Figs. 4(a) and 4(b) (empty In and filled Sb state density, respectively). Note the "×" ("O") in Fig. 4(a) [4(b)] indicating the position of the Sb (In) vacancy in Fig. 4(b) [4(a)]. As a neutral defect, considerably less charge redistribution is expected around a Schottky defect compared with a charged anion vacancy; as indicated by the variations in "height" of the dangling bonds surrounding the vacancies, less perturbation is observed. In contrast to the relatively long-range perturbations induced by an isolated anion vacancy, only the surface atoms immediately adjacent to the Schottky defect are affected, with some appearing slightly raised. Again, this may be due to

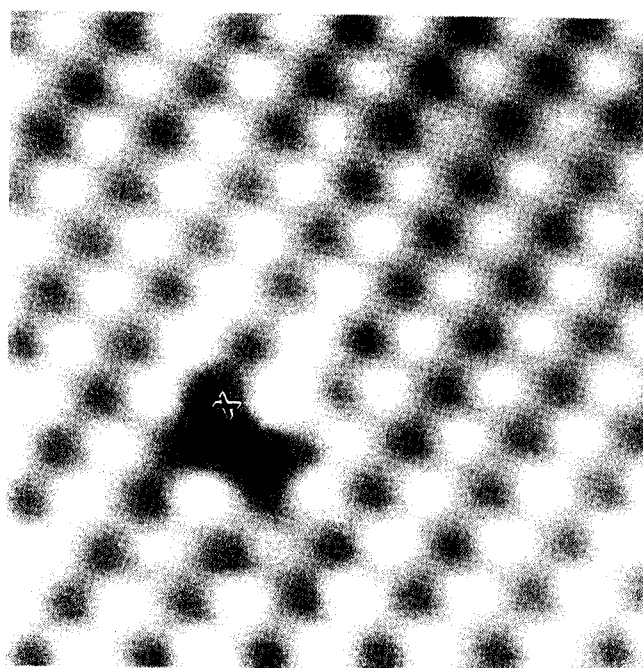


(a)

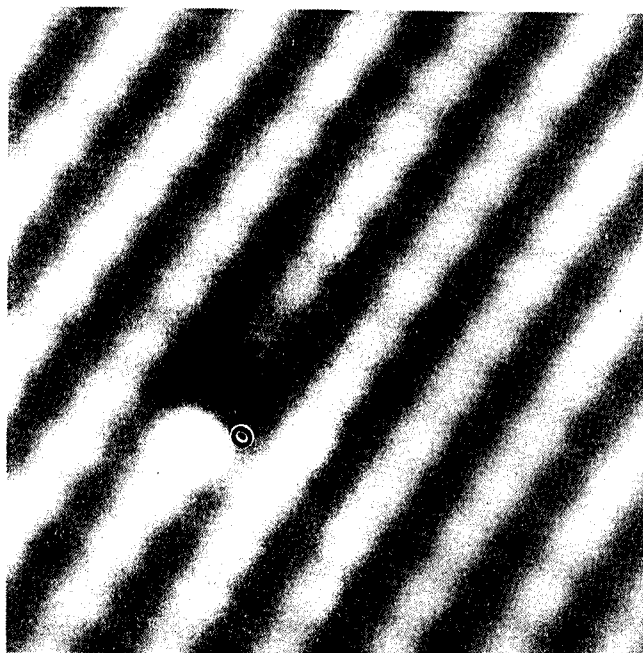
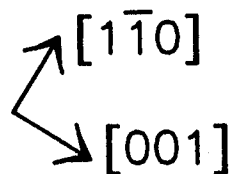


(b)

FIG. 3. A pair of 45×45 -Å gray-scale topographic images of a defect on InSb(110). The images were recorded simultaneously with sample bias voltages of (a) + 1.2 V (In state density) and (b) - 1.0 V (Sb state density). The defect appears to be a simple anion (Sb) vacancy. The "×" in (a) indicates the position of the Sb atom missing in (b). Note the perturbations surrounding the defect are asymmetrical in both crystallographic directions. See text for discussion.



(a)



(b)

FIG. 4. A pair of 45×45 -Å gray-scale topographic images of InSb(110) recorded simultaneously with sample bias voltages of (a) $+1.3$ V (In state density) and (b) -1.1 V (Sb state density) showing a different type of defect than that observed in Fig. 3. This defect appears to consist of adjacent In and Sb vacancies, i.e., a Schottky defect. The "x" ("O") in (a) [(b)] indicates the position of the Sb (In) missing in (b) [(a)]. Note that the asymmetrical perturbations surrounding this neutral defect are less severe than those surrounding the charged anion vacancy (Fig. 3).

charge redistribution and/or outward relaxation of the atoms surrounding the vacancies. We also find the surface perturbations induced by Schottky defects to be asymmetrical along both crystallographic directions, though less dramatically so than around anion vacancies. For a Schottky defect the asymmetries are at least in part associated with the relative orientation of the vacancy pair; the In (Sb) adjacent in the row to the missing Sb (In) always appears "raised."

As discussed above, an important reason for studying InSb(110) was to determine the Cs structures observed following room-temperature adsorption. As is evident from Fig. 5, Cs forms long zig-zag chains along $[1\bar{1}0]$ on InSb(110) like those observed on GaAs(110).^{17,18} This structure, with a large Cs-Cs nearest-neighbor distance of 8.0 Å (compared with 6.9 Å on GaAs), is surprising since the Cs-Cs distance in a straight chain configuration, 4.6 Å, would be closer to the bulk Cs-Cs distance of 5.2 Å. Evidently the driving force for the formation of the zig-zag structure is significant. The formation of these structures also indicates that the adsorbed Cs is highly mobile on these room-temperature surfaces, and that the Cs-Cs interaction is anisotropically dominated by attractive interactions along the $[1\bar{1}0]$ chain direction.

Further study reveals that the Cs adsorbed on InSb(110) differs in a number of ways from Cs adsorbed on GaAs(110). First, for a given Cs coverage the chains observed on InSb(110) tend to be shorter than those on GaAs(110), and the extremely long chains (> 2000 Å) formed on GaAs (Ref. 18) are not found on InSb. In addition, the Cs chains on InSb(110) are almost always terminated on one end by the large structures observed as high

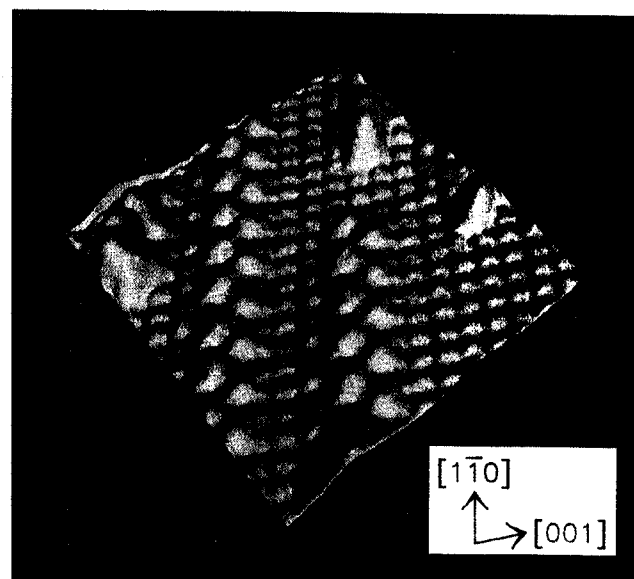


FIG. 5. An approximately 90×90 -Å topographic image of the occupied state density (sample bias voltage of -2.3 V) acquired following Cs adsorption on room-temperature InSb(110). The image is shown in perspective with specular illumination. The one-dimensional zig-zag chains formed by Cs, similar to those previously observed on GaAs(110), are clearly resolved, as are the substrate Sb atom dangling bonds. The Cs nearest-neighbor distance in this structure is 8.0 Å. The large structures which terminate many of the chains are believed to be three-dimensional Cs clusters.

points in Fig. 5. We believe these are Cs clusters adsorbed on top of the ends of Cs zig-zag chains. Close examination of the structure at the top of Fig. 5, for instance, reveals a dimerlike twin-peaked structure with maxima located where the hollows between the underlying Cs atoms are expected to be. We do not believe these are contaminant adsorbates, since they are not observed when Cs is adsorbed on GaAs(110) under similar vacuum conditions, and their density does not increase with time. One possibility is that the larger lattice constant of InSb reduces the stability of the chains, resulting in shorter chains which tend to "ball up" on the ends in order to compensate for the intrinsic instability associated with chain termination. As will be described in detail elsewhere,¹⁸ tunneling current-versus-bias voltage measurements reveal that the chains are nonmetallic (no density of states at the Fermi level) on both InSb(110) and GaAs(110).

IV. CONCLUSIONS

We have employed scanning tunneling microscopy to obtain atomic resolution images of both the filled and empty electronic state densities on InSb(110). From the relative positions of the empty and filled dangling bonds observed in simultaneously acquired images, the surface buckling has been determined, and is found to be in good agreement with that predicted by calculations. Both simple anion (Sb) vacancies and adjacent Sb and In vacancies (Schottky defects) have been observed. The charged anion vacancies result in anisotropic surface relaxation and/or charge redistribution of the surrounding atoms, with the perturbation in the [001] direction longer ranged than in [00 $\bar{1}$]. In addition, an asymmetrical buckling of the atoms adjacent (in the row along [1 $\bar{1}$ 0]) to each Sb vacancy site has been observed; this is surprising since these atoms on either side of the vacancy are in principle equivalent. Similar perturbations are observed surrounding the Schottky defects, though fewer neighboring atoms are affected and the perturbations are smaller, as might be expected for a neutral-versus-charged defect.

Cs adsorbed on room-temperature InSb(110) forms long one-dimensional zig-zag chains along [1 $\bar{1}$ 0], similar to those previously observed on GaAs(110).^{17,18} The formation of these structures demonstrates that Cs is highly mobile, with Cs-Cs interactions dominated by attractive forces along [1 $\bar{1}$ 0]. The chains are shorter on InSb than GaAs, probably due to the larger Cs-Cs nearest-neighbor distance.

ACKNOWLEDGMENTS

We would like to thank S. Mielczarek and R. Cutkosky for expert technical assistance, and gratefully acknowledge the partial support of the Office of Naval Research. L. J. Whitman is a National Research Council Postdoctoral Research Associate.

- ¹C. Y. Wei, K. L. Wang, E. A. Taft, J. M. Swab, M. D. Gibbons, W. E. Davern, and D. M. Brown, *IEEE Trans. Electron Devices* **27**, 170 (1980).
- ²K. Asauskas, Z. Dobrovolskis, and A. Krotkus, *Sov. Phys. Semicond.* **14**, 1377 (1980).
- ³C. B. Duke, R. J. Meyer, A. Paton, J. L. Yeh, J. C. Tsang, A. Kahn, and P. Mark, *J. Vac. Sci. Technol.* **17**, 501 (1980); R. J. Meyer, C. B. Duke, A. Paton, J. L. Yeh, J. C. Tsang, A. Kahn, and P. Mark, *Phys. Rev. B* **21**, 4740 (1980).
- ⁴J. Bohr, R. Feidenhans'l, M. Nielsen, M. Toney, R. L. Johnson, and I. K. Robinson, *Phys. Rev. Lett.* **54**, 1275 (1985).
- ⁵E. W. Kreutz, E. Rickus, and N. Sotnik, *Surf. Sci.* **151**, 52 (1985), and references therein.
- ⁶I. Hernández-Calderón, *Surf. Sci.* **152/153**, 1130 (1985); H. Höchst and I. Hernández-Calderón, *J. Vac. Sci. Technol. A* **3**, 911 (1985), and references therein.
- ⁷H. Lüth, *Surf. Sci.* **168**, 773 (1986), and references therein.
- ⁸V. A. Grazulis, *Appl. Surf. Sci.* **33/34**, 1 (1988).
- ⁹C. M. Aldao, I. M. Vitomirov, F. Xu, and J. H. Weaver, *Phys. Rev. B* **40**, 3711 (1989).
- ¹⁰B. M. Tefas, C. M. Aldao, C. Capasso, Yoram Shapira, F. Boscherini, I. M. Vitomirov, and J. H. Weaver, *Phys. Rev. B* **40**, 9811 (1989).
- ¹¹Liang *et al.* have also been studying InSb(110) with STM; see Y. Liang, W.-M. Hu, W. E. Packard, and J. D. Dow, *Bull. Am. Phys. Soc.* **35**, 227 (1990).
- ¹²W. A. Goddard III, J. J. Barton, A. Redondo, and T. C. McGill, *J. Vac. Sci. Technol.* **15**, 1274 (1978).
- ¹³A. R. Lubinsky, C. B. Duke, B. W. Lee, and P. Mark, *Phys. Rev. Lett.* **36**, 1058 (1976).
- ¹⁴J. R. Chelikowski and M. L. Cohen, *Solid State Commun.* **29**, 267 (1979).
- ¹⁵J. Tersoff and D. R. Hamann, *Phys. Rev. B* **31**, 805 (1985).
- ¹⁶R. M. Feenstra, Joseph A. Stroscio, J. Tersoff, and A. P. Fein, *Phys. Rev. Lett.* **58**, 1192 (1987).
- ¹⁷P. N. First, R. A. Dragoset, Joseph A. Stroscio, R. J. Celotta, and R. M. Feenstra, *J. Vac. Sci. Technol. A* **7**, 2868 (1989).
- ¹⁸L. J. Whitman, Joseph A. Stroscio, R. A. Dragoset, and R. J. Celotta (to be published).
- ¹⁹G. Binnig and H. Rohrer, *Sci. Am.* **253**, 50 (1985).
- ²⁰R. D. Cutkosky, *Rev. Sci. Instrum.* **61**, 960 (1990).
- ²¹C. Mailhot, C. B. Duke, and D. J. Chadi, *Surf. Sci.* **149**, 366 (1985).
- ²²L. J. Whitman, Joseph A. Stroscio, R. A. Dragoset, and R. J. Celotta, *Phys. Rev. B* **42**, 7288 (1990).
- ²³J. Tersoff (private communication).
- ²⁴See, for instance, R. Cotterill, *The Cambridge Guide to the Material World* (Cambridge University Press, Cambridge, 1985), p. 76.